Supplementary Materials for

Abberant oligodendroglial LDL receptor orchestrates demyelination in chronic cerebral ischemia

Yi Xie,† Xiaohao Zhang,† Pengfei Xu,† Nana Zhao, Ying Zhao, Yunzi Li, Ye Hong, Mengna Peng, Kang Yuan, Ting Wan, Rui Sun, Deyan Chen, Lili Xu, Jingjing Chen, Hongquan Guo, Wanying Shan, Juanji Li, Rongrong Li, Yunyun Xiong, Dezhi Liu, Yuhui Wang, George Liu, Ruidong Ye,* Xinfeng Liu*

†Contributed equally.

*Corresponding author. E-mail: xfliu2@vip.163.com (X.L.); yeruid@gmail.com (R.Y.)

The file includes:

Methods

Antibodies. Antibodies against AIF (ab1998), β3-tubulin (ab78078), CNPase (ab6319), GFAP (ab53554), HIF-1α (ab1), Ki67 (ab15580), LC3-B (ab48394), MAG (ab89780), MBP (ab40390), NF200 (ab7795), PLP (ab28486) were purchased from Abcam, UK; antibodies against GFP (2956S/2955S), Shc (2432), p-Shc (2434), MEK1/2 (4694), p-MEK1/2 (9154), ERK1/2 (4695), p-ERK1/2 (4370), β-actin (8457) were purchased from Cell Signaling Technology, USA; antibody against GST-pi (MBL 312) was purchased from MBL corporation, Japan; antibodies against CC1 (OP80), NG2 (MAB5384), Olig2 (AB9610) were purchased from Millipore, USA; antibodies against LDLR (AF2255-SP), O4 (MAB1326-SP) were purchased from R&D Systems, USA; antibody against LDLR (sc-11824), PDGFR-α (sc-398206) were purchased from Santa Cruz Biotechnology, USA; antibody against A2B5 (A8229) was purchased from Sigma-Aldrich, USA. All antibodies were used at a dilution of 1:50–1:500 for immunofluorescence, 1:500–1:1000 for immunoblotting analysis unless otherwise specified. Secondary antibodies were donkey-anti-mouse, or anti-rabbit, or anti-goat conjugated with either Alexa 488 or Alexa 594 or Alexa 647 (Jackson, USA; 1:400), goat anti mouse or rabbit IgG HRP (Cell Signaling Technology, USA; 1:5000).

Culture conditions. For mixed glial, astrocytic and microglial culture, cells were maintained in DMEM/F12 medium with 10% FBS and 1% PS. For OPCs proliferation, cells were replated in DMEM/F12 medium with 20 ng ml^{-1} PDGF (Biolegend), 20 ng ml^{-1} bFGF (Biolegend), 20ng ml^{-1} ITSS (Roche) and 1% BSA (Gibco). For OPCs differentiation, the culture medium was switched to DMEM/F12 containing 40 ng ml^{-1}

T3 (Sigma), 20 ng ml^{-1} CNTF (Protein specialists), 1× N-acetyl-L-cysteine (NAC, Sigma), 20 ng ml^{-1} ITSS and 1% BSA supplement. For myelination coculture system, maintenance medium was consisted of neurobasal (Gibco) containing 2% B27, and 1% GlutaMAX (Gibco). Myelin coculture medium contained OPCs proliferation or differentiation medium and maintenance medium with the ratio of 1:1.

Human MRI assessment. We defined leukoaraiosis as hyperintense lesions on axial T2 fluid-attenuated inversion recovery (FLAIR) images that are located in the region starting at the lateral ventricular border and extending up to the corticomedullary junction (GM Kim et al., 2014). All MRI scans were rated by who were blinded to the clinical data. Limited intra-rater reliability testing (50 patients) demonstrated a good reliability with kappa values of 0.88 for the diagnosis of leukoaraiosis. Any discrepancy with regard to the diagnosis of the leukoaraiosis was resolved by consensus between the readers after reviewing the MRI films again. Finally, 118 patients with leukoaraiosis and 69 subjects without leukoaraiosis were finally included in this study.

Mice DTI imaging. Mice were anesthetized (2.5% isoflurane at 2.5 L/min oxygen) and wrapped with a hot-water-circulated blanket to maintain their temperature through the scanning. Breathing and heart rate were continuously monitored at the same time. MR scans were obtained using a TurboRARE-T2 pulse sequence [repetition time (TR) = 3000 ms, echo times (TEs) = 36.0 ms, slice thickness = 1 mm, field of view (FOV) = 2.0 × 2.0 cm^2, 256 × 256 matrix, number of excitation (NEX) = 1].

Diffusion tensor image (DTI) was acquired using an echo planar imaging (EPI) diffusion tensor sequence (TR = 5000 ms, TEs = 32.2 ms, slice thickness = 0.6 mm, FOV = 2.0 × 2.0 cm^2, 128 × 128 matrix, NEX = 2 and a b-factor = 1000 s/mm^2). Fiber trajectories and FA values in the CC were taken from four regions of interest (ROIs), which were at slice positions 1.2, 0.6, −0.6, and −1.2 mm anterior to the bregma. Tractographies were displayed by a directional coloring code: red for left–right, blue for cranial–caudal, and green for dorsal–ventral directions.

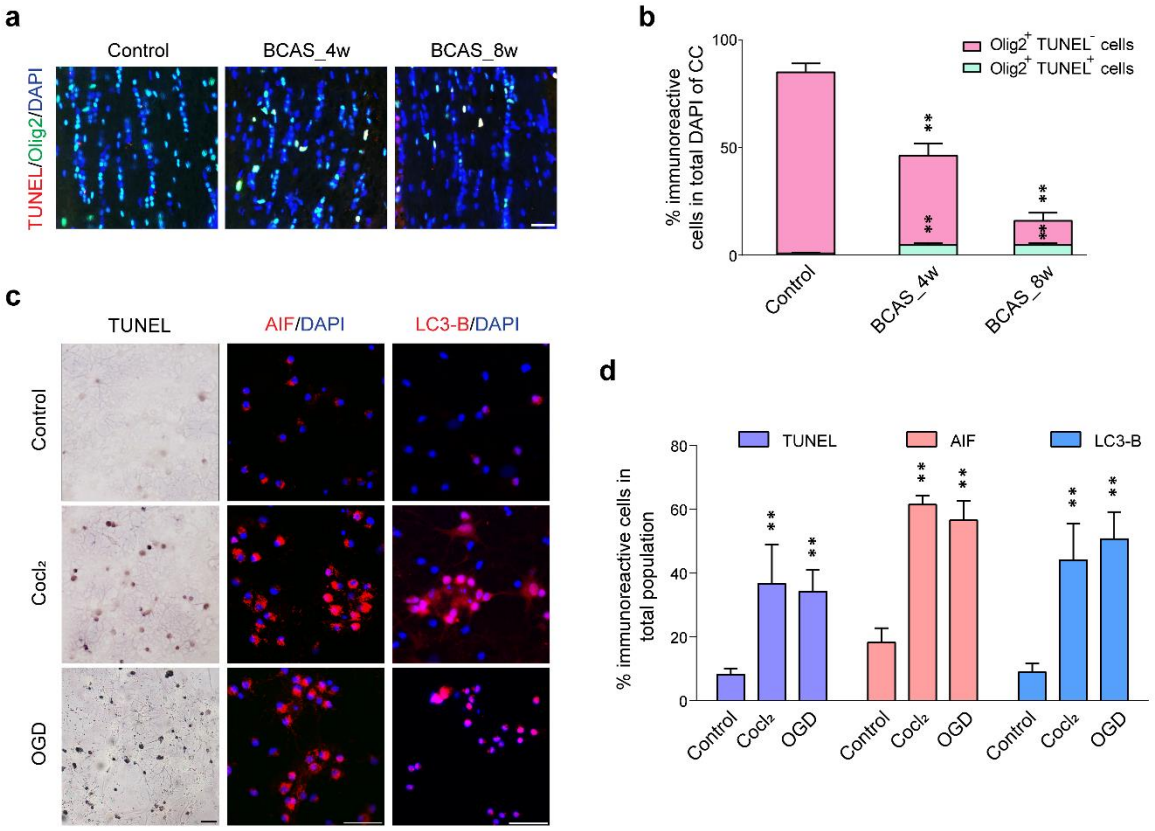

Supplemental Figure 1. Oligodendroglial cell death after hypoxic-ischemic injury. (**a,b**) *In vivo* oligodendroglial apoptosis was observed in BCAS mice (n = 4 in each group; mean ± S.D.; ***P* < 0.01 *vs* controls; one-way ANOVA, Tukey post hoc test). (**c,d**) *In vitro* oligodendroglial cell death stained with TUNEL (apoptosis marker), AIF (parthanatos marker), LC3-B (autophagy-related protein) were caused by hypoxic treatment (n = 4 experiments; mean ± S.D.; ***P* < 0.01 *vs* controls; one-way ANOVA, Tukey post hoc test). Scale bar, 20 μm.

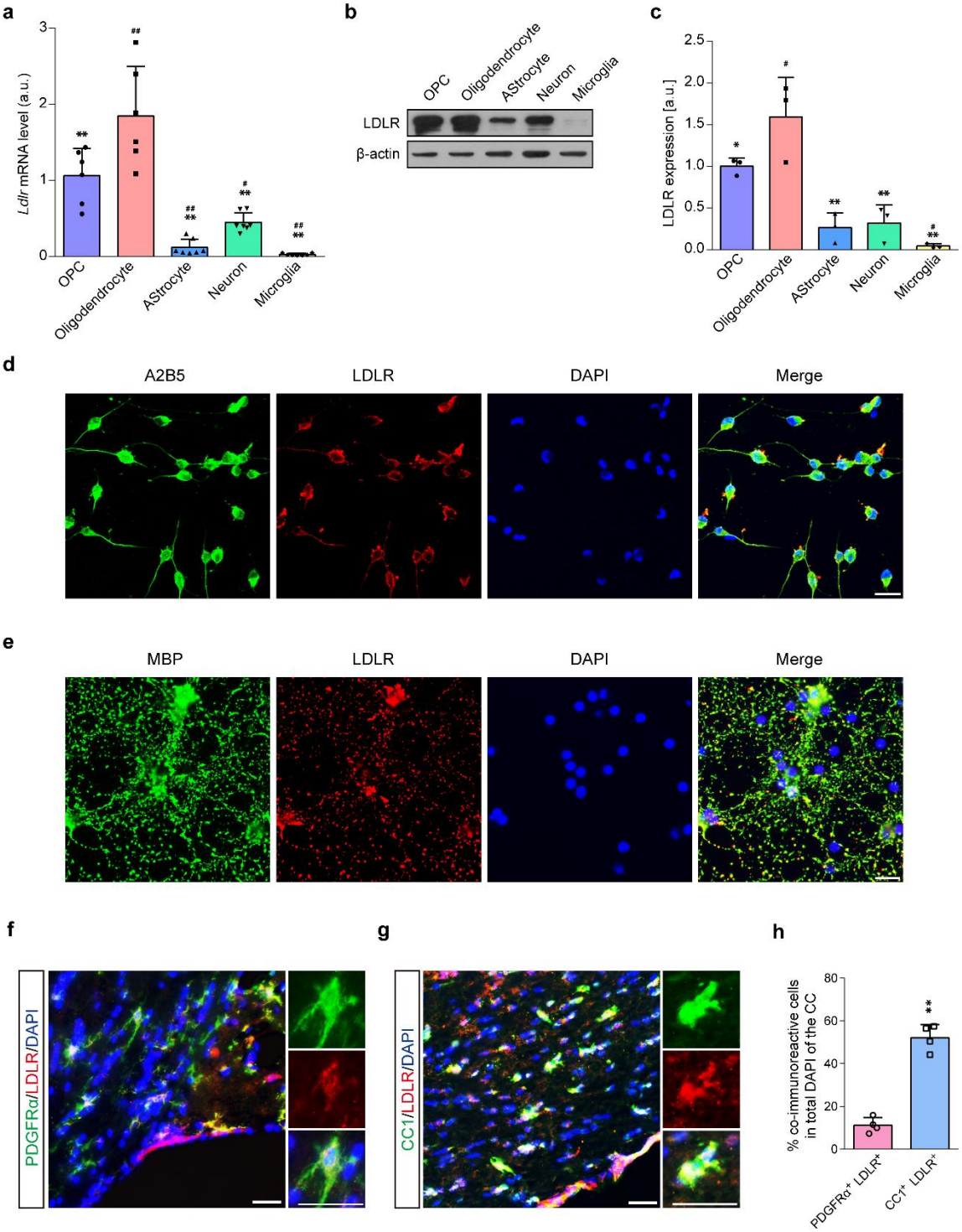

Supplemental Figure 2. Specific expression of LDLR in neural cells. (**a–c**) LDLR mRNA and protein levels in OPC, oligodendrocyte, astrocyte, neuron and microglia (n ≥ 3 experiments; mean ± S.D.; $^{\#}P < 0.05$, $^{\#\#}P < 0.01$ *vs* OPC, $^{*}P < 0.05$, $^{**}P < 0.01$ *vs* oligodendrocyte; one-way ANOVA, Tukey post hoc test). (**d,e**) Representative immunofluorescent images of LDLR staining in OPC and oligodendrocyte *in vitro* (n = 4 experiments). (**f,g**) Representative immunofluorescent images of LDLR staining in OPC and oligodendrocyte *in vivo* [n = 4 in each group; mean ± S.D.; $^{**}P < 0.01$ *vs* PDGFRα^{+}LDLR^{+} cells; paired *t*-test, quantified in (**h**)]. Scale bar: 20 µm.

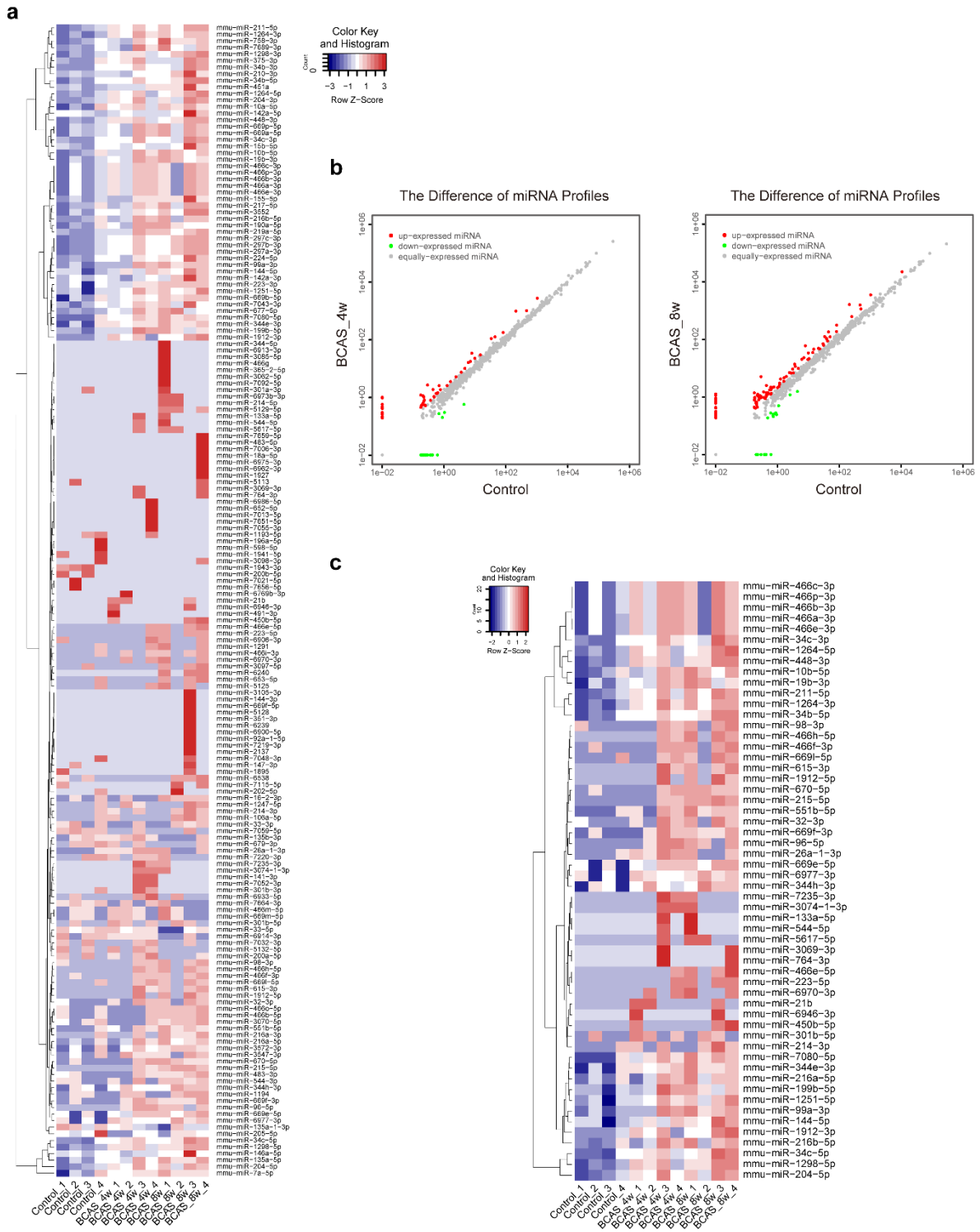

Supplemental Figure 3. Systematic screening of miRNAs expression in the CC of BCAS mice. (**a**) A total of 175 miRNAs were changed during the pathological process of chronic cerebral ischemia with a fold change > 2. (**b**) Volcano plots of high-throughput sequencing of miRNA in BCAS_4w and BCAS_8w respectively. (**c**) Among those altered miRNAs, 65 miRNAs were both elevated in BCAS_4w and BCAS_8w groups. (n = 4 in each group)

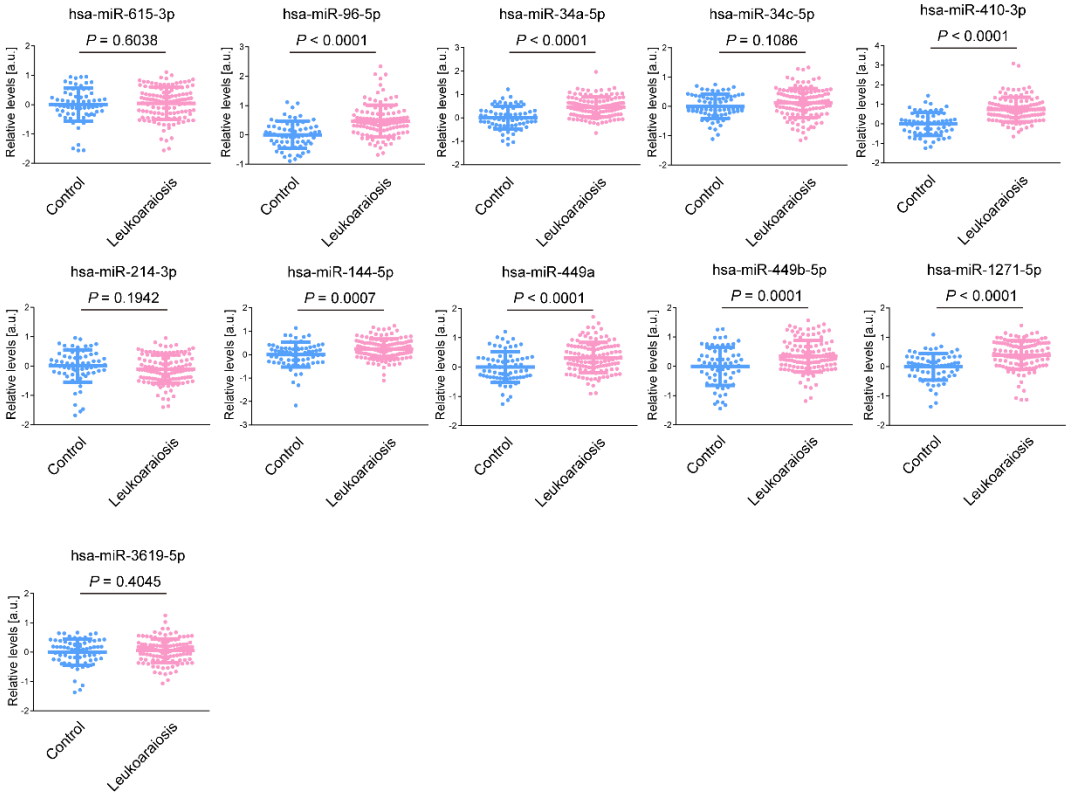

Supplemental Figure 4. Log-transformed serum miRNAs levels of control and patients with leukoaraiosis. Eleven miRNAs sharing common seed sequences with thirteen mouse miRNAs were chosen. Ct value of each miRNA was normalized to that of C. *elegans* miR-39-3p. Each point represents the mean of triplicate repeat (n = 69 in control, n = 118 in case; mean ± S.D.; unpaired *t*-test).

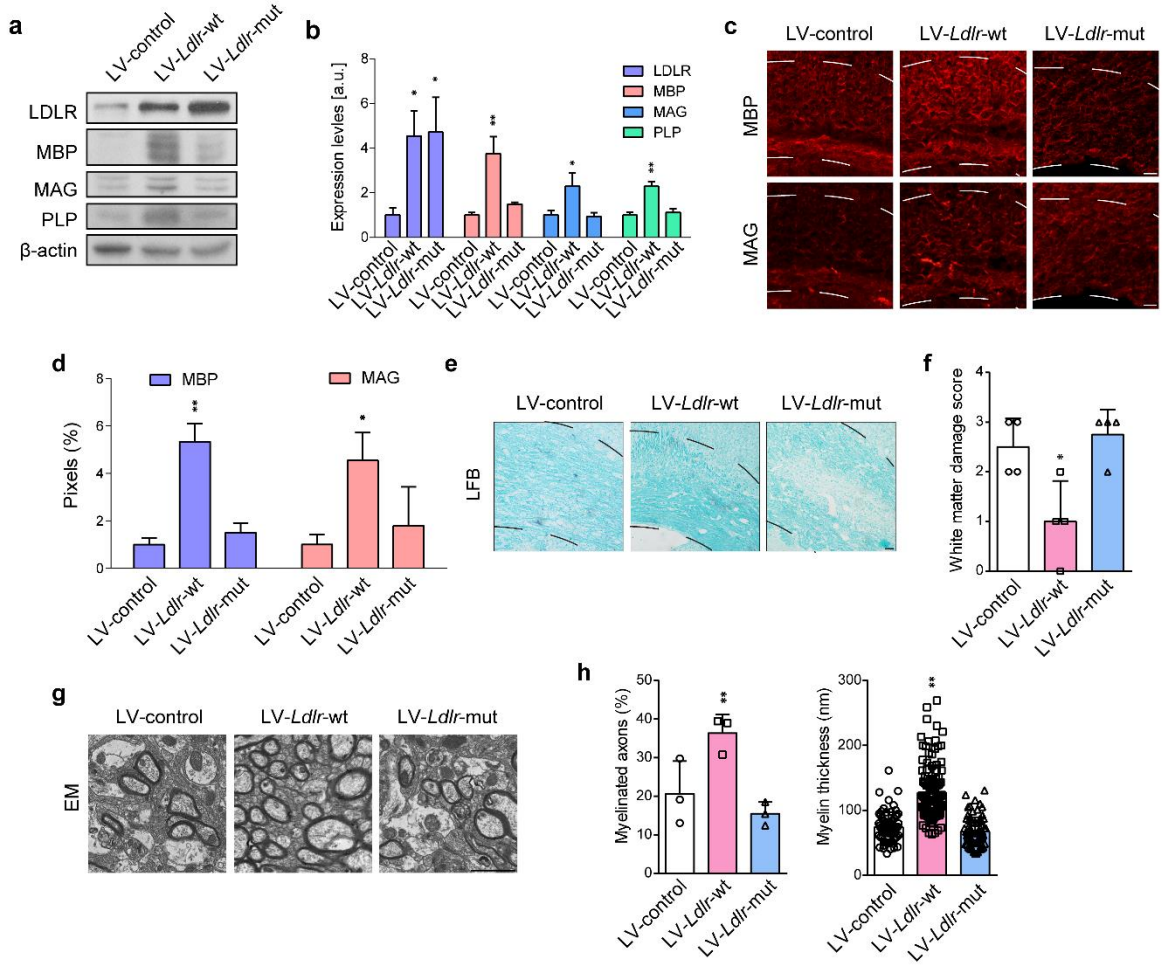

Supplemental Figure 5. The protection of wild type LDLR lasts up to 8 weeks after BCAS. (**a**) Western blotting showing the expression of LDLR and myelin proteins [n = 3 experiments; mean ± S.D.; **P* < 0.05, ***P* < 0.01 *vs* LV-control; one-way ANOVA, Tukey post hoc test, quantified in (**b**)]. (**c–h**) Representative MBP, MAG, LFB staining, EM images and quantifications of the CC from BCAS mice receiving lentivirus encoding null, wild type and mutated *Ldlr* (n ≥ 3 in each group; mean ± S.D.; **P* < 0.05, ***P* < 0.01 *vs* LV-control; one-way ANOVA, Tukey post hoc test). The CC boundary is indicated by the dashed line. Scale bar: 2 μm in EM or 20 μm in others.

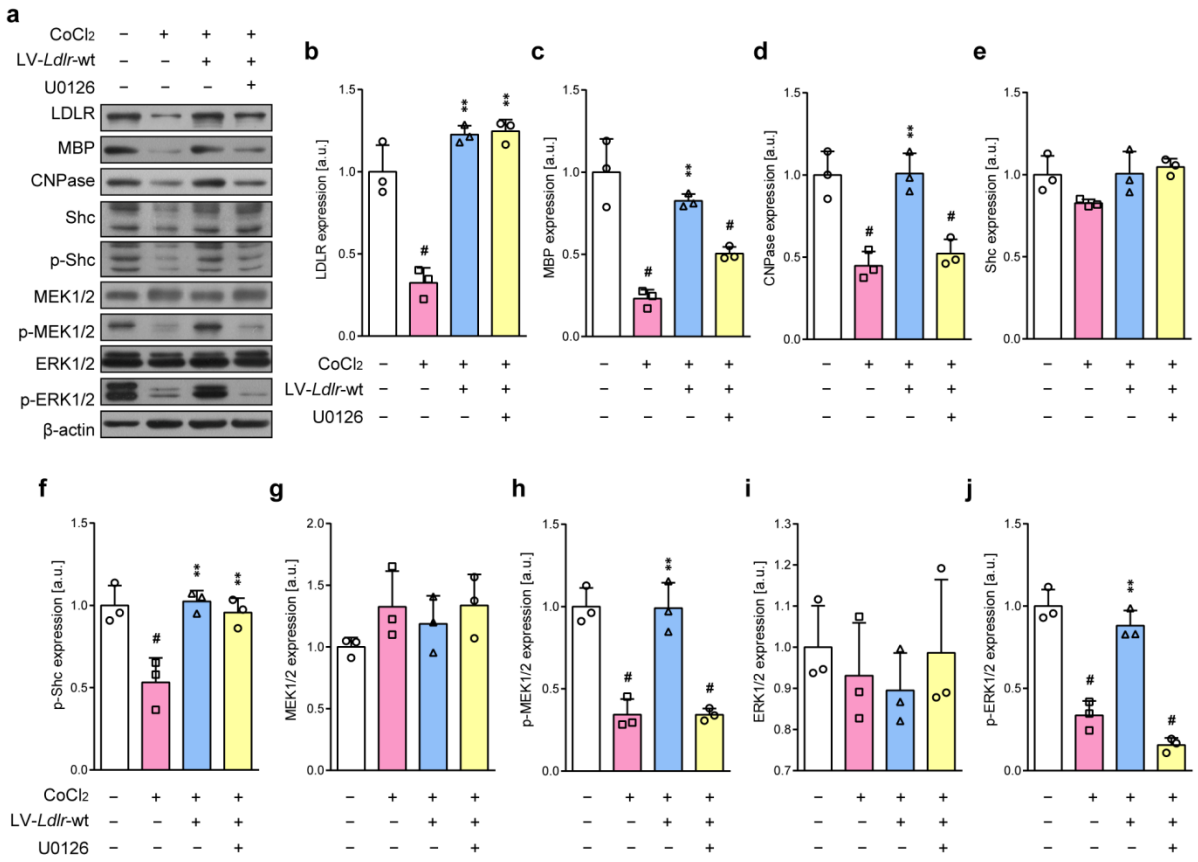

Supplemental Figure 6. U0126 abolishes LDLR-induced attenuation of myelin protein expression and signaling activation in hypoxia. Immunoblotting and quantifications for LDLR, myelin-associated proteins (MBP, CNPase) and molecules (Shc/p-Shc, MEK/p-MEK, ERK/p-ERK) in Shc/MEK/ERK pathway (n = 3 experiments; mean ± S.D.; $^{\#}P < 0.05$ *vs* controls, $^{*}P < 0.05$, $^{**}P < 0.01$ *vs* $CoCl_2$-treated cells; one-way ANOVA, Tukey post hoc test).

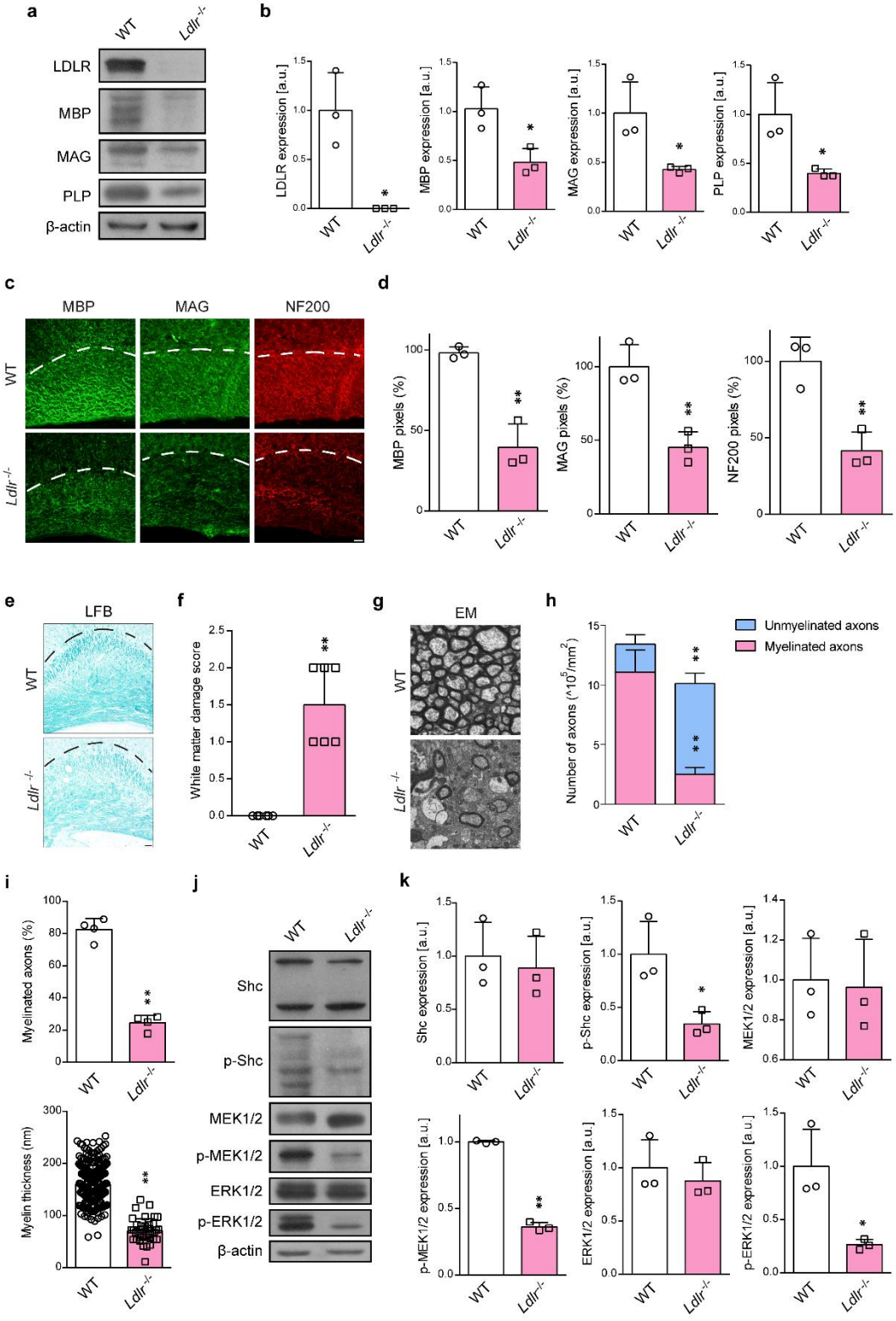

Supplemental Figure 7. *Ldlr*$^{-/-}$ mice displays hypomyelination in the CC. (**a**,**b**) Immunoblotting and statistical analyses of the expression of LDLR and myelin proteins (n = 3 in each group; mean ± S.D.; **P* < 0.05 *vs* wild type mice, paired *t*-test). (**e**) MBP, MAG, NF200, (**e**) LFB staining and (**g**) EM images taken from the CC of wild type and *Ldlr*$^{-/-}$ mice [n ≥ 3 in each group; mean ± S.D.; ***P* < 0.01 *vs* wild type mice, paired *t*-test, quantified in (**f**,**h**,**i**)]. The CC boundary is indicated by the dashed line. (**j**) Immunoblotting of the expression of

Shc/MEK/ERK pathway [n = 3 in each group; mean ± S.D.; *$P < 0.05$, **$P < 0.01$ *vs* wild type mice, paired *t*-test, quantified in (**k**)]. Scale bar: 2 μm in EM or 20 μm in others.

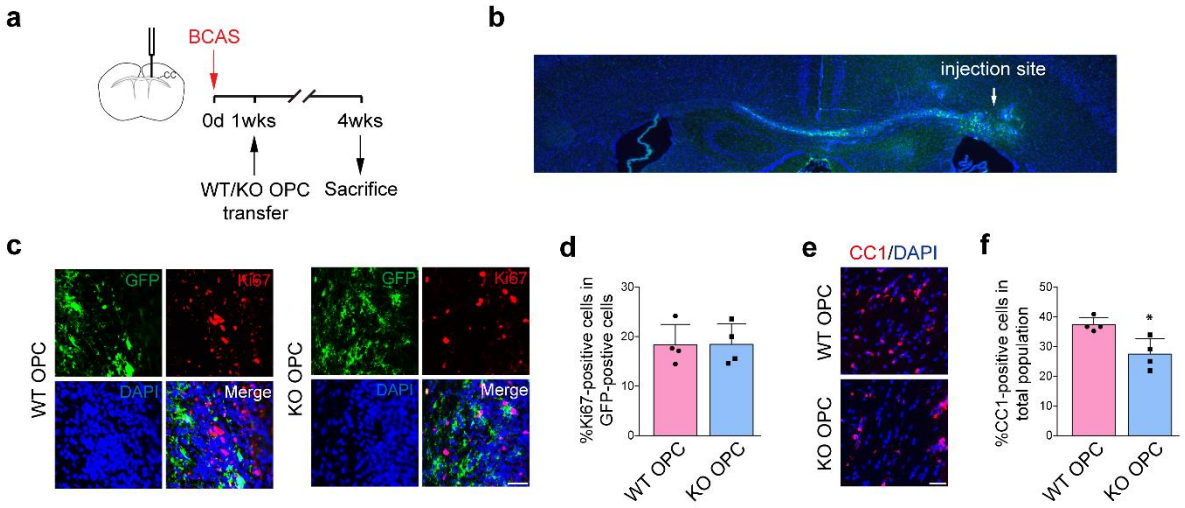

Supplemental Figure 8. The migration and proliferation of transplanted OPCs and the number of myelinating oligodendrocytes in the CC adjacent to transplantation. (**a**) Experimental flow chart. (**b**) Fluorescent image showing the migration along the CC from injection site. (**c,d**) Fluorescent images and quantification of proliferated exogenous OPCs (n = 4 in each group; mean ± S.D.; unpaired *t*-test). (**e,f**) Fluorescent images and quantification of $CC1^+$ mature oligodendrocytes in area adjacent to injection site (n = 4 in each group; mean ± S.D.; **P* < 0.05 *vs* wild type OPC, unpaired *t*-test). Scale bar: 20 μm.

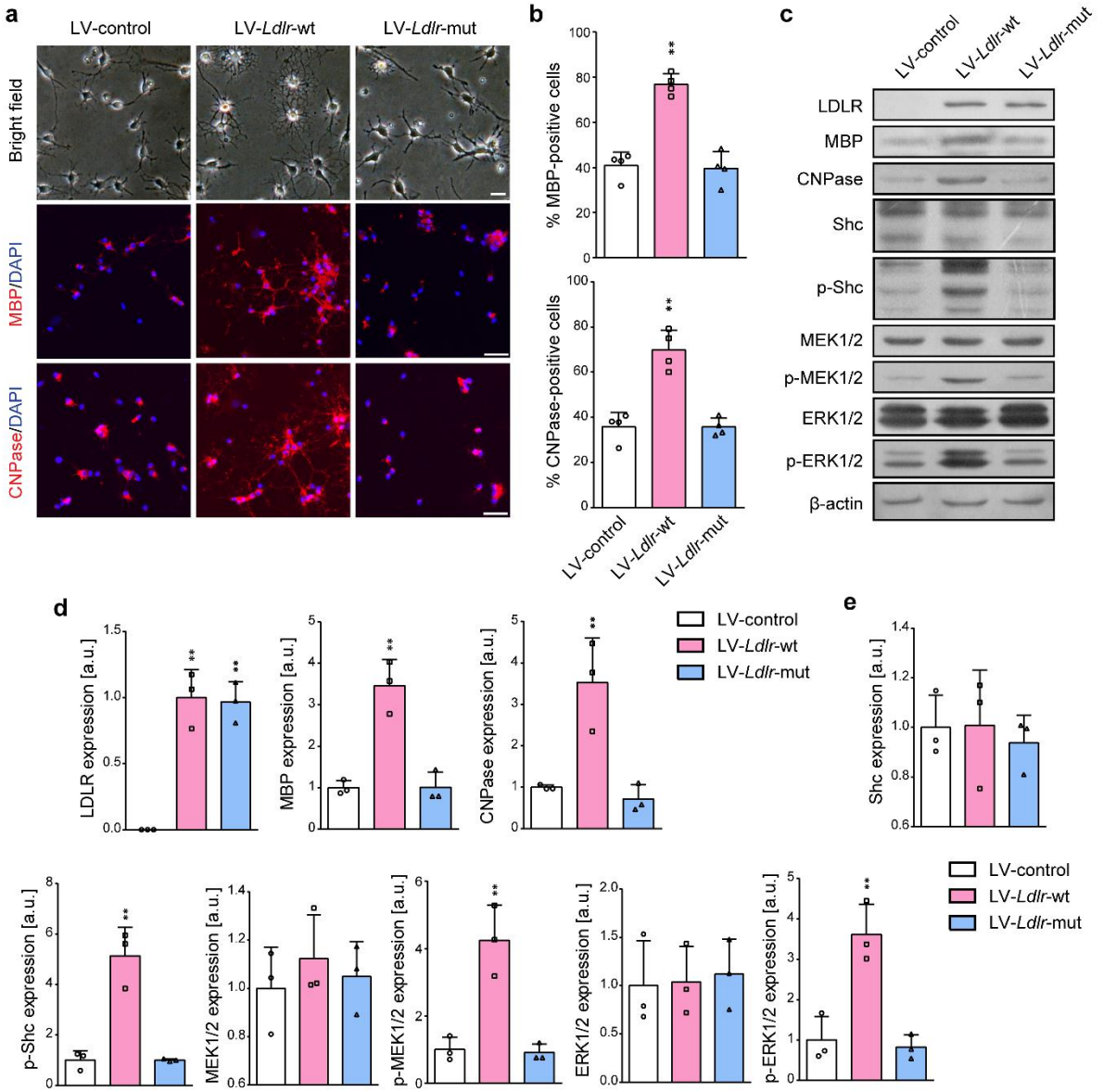

Supplemental Figure 9. Re-expression of LDLR with NPVY motif promotes the differentiation of *Ldlr*$^{-/-}$ OPCs. (**a**) Representative light microscopic photos, MBP and CNPase staining images of *Ldlr*$^{-/-}$ oligodendrocytes transfected with null, wild type and mutated *Ldlr*:GFP reporter viruses [n = 4 experiments; mean ± S.D.; ***P* < 0.01 *vs* LV-control; one-way ANOVA, Tukey post hoc test, quantified in (**b**)]. (**c**) Immunoblotting demonstration of LDLR, myelin-related proteins and Shc/MEK/ERK signaling expressions. (**d,e**) Scatter plot histogram analysis of the expression of LDLR, myelin proteins and molecules in Shc/MEK/ERK signaling (n = 3 experiments; mean ± S.D.; ***P* < 0.01 *vs* LV-control; one-way ANOVA, Tukey post hoc test). Scale bar: 20 μm.

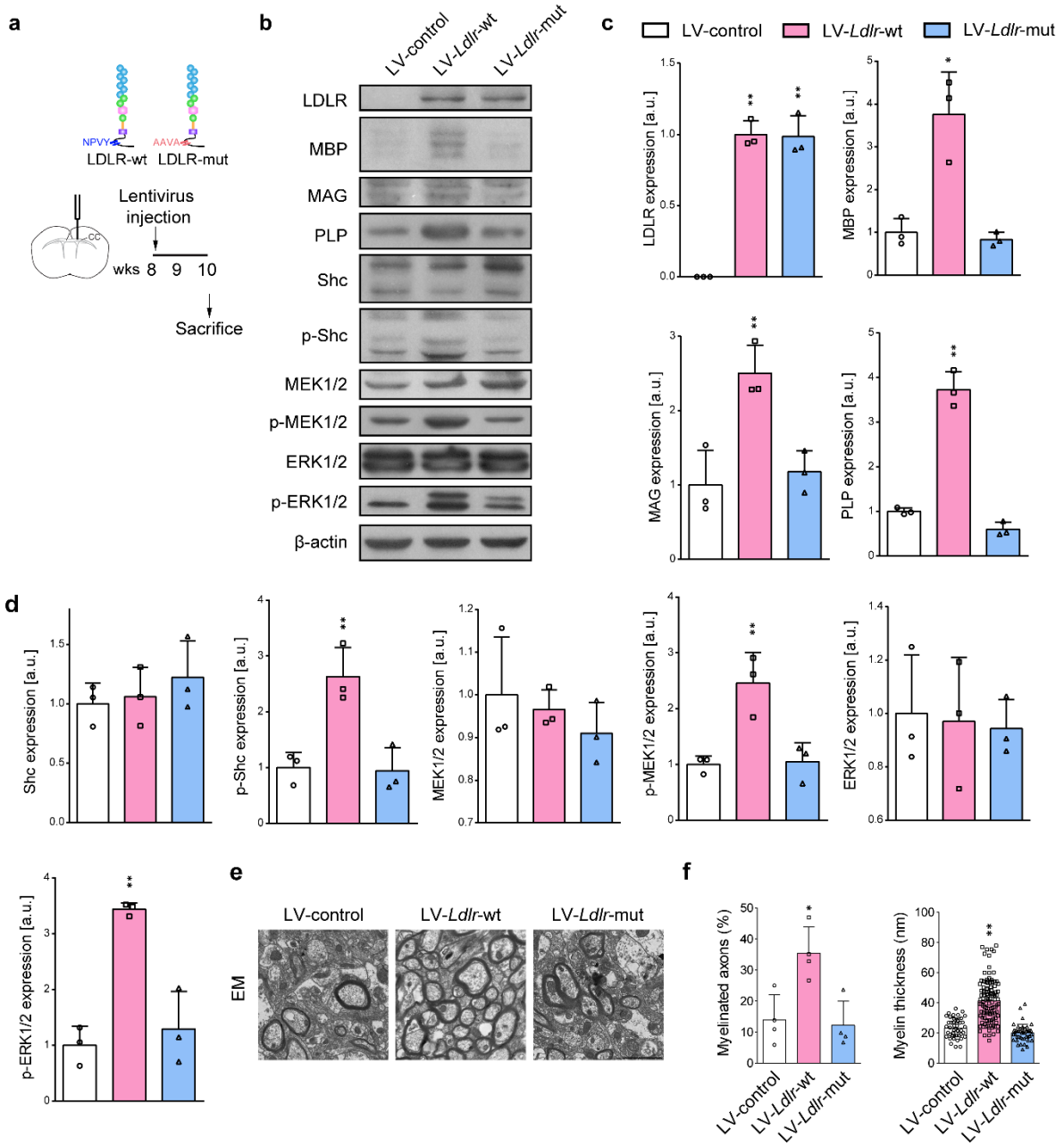

Supplemental Figure 10. Re-expression of LDLR with NPVY motif preserves myelin protein expression and myelin microstructure in *Ldlr*$^{-/-}$ mice. (**a**) Experimental flow chart. (**b**) Immunoblotting demonstrations of LDLR, myelin proteins and Shc/MEK/ERK pathway [n = 3 in each group; mean ± S.D.; **P* < 0.05, ***P* < 0.01 *vs* LV-control, one-way ANOVA, Tukey post hoc test, quantified in (**c,d**)]. (**e**) EM images obtaining from the CC of KO mice receiving lentiviruses [n = 4 in each group; mean ± S.D.; **P* < 0.05, ***P* < 0.01 *vs* LV-control; one-way ANOVA, Tukey post hoc test, quantified in (**f**)]. Scale bar, 2 μm.

Supplemental Table 1. miRNAs sharing the same seed region in rodents and human.

Seed region sequence	mice	rat	human
CCGAGCC	mmu-miR-615-3p	none	hsa-miR-615-3p
UUGGCAC	mmu-miR-96-5p	rno-miR-96-5p	hsa-miR-96-5p hsa-miR-1271-5p
AUAUAAC	mmu-miR-344e-3p	rno-miR-344b-1-3p rno-miR-410-3p	hsa-miR-410-3p
GGCAGUG	mmu-miR-34b-5p mmu-miR-34c-5p	rno-miR-34b-5p rno-miR-34c-5p	hsa-miR-34a-5p hsa-miR-34c-5p hsa-miR-449a hsa-miR-449b-5p
CAGCAGG	mmu-miR-214-3p	rno-miR-214-3p	hsa-miR-214-3p hsa-miR-3619-5p
GAUAUCA	mmu-miR-144-5p	rno-miR-144-5p	hsa-miR-144-5p
ACAGAAC	mmu-miR-1912-3p	rno-miR-1912-3p	none
GUCUUGU	mmu-miR-669e-5p	rno-miR-331-5p	none
AUAUACA	mmu-miR-669f-3p	none	none
AUACAUA	mmu-miR-466a-3p/466e-3p	none	none
AUGUGUG	mmu-miR-466e-5p	rno-miR-466b-5p	none

Supplemental Table 2. Logistic regression analysis for associated factors with leukoaraiosis.

Variables	Univariate logistic regression analysis		Multivariate logistic regression analysis	
	OR (95% CI) for WMLs	*P* value	OR (95% CI) for WMLs	*P* value
Age	1.084 (1.043–1.126)	0.001	1.080 (1.021–1.143)	0.007
Male	1.312 (0.714–2.411)	0.382		
Hypertension	3.217 (1.684–6.145)	0.001	2.199 (0.819–5.905)	0.118
Diabetes mellitus	2.625 (1.268–5.434)	0.009	1.141 (0.381–3.418)	0.814
Hyperlipidemia	0.850 (0.442–1.636)	0.627		
miRNAs of interest (log-transformed)				
hsa-miR-410-3p	9.345 (4.340–20.121)	0.001	5.756 (2.069–16.010)	0.001
hsa-miR-34a-5p	10.769 (4.610–25.156)	0.001	3.733 (1.032–13.507)	0.045
hsa-miR-1271-5p	1.508 (1.254–1.814)	0.001	2.603 (0.777–8.724)	0.121
hsa-miR-96-5p	7.910 (0.001–0.004)	0.001	2.908 (0.810–10.583)	0.101
hsa-miR-449b-5p	2.756 (1.594–4.763)	0.001	1.931 (0.617–6.042)	0.258
hsa-miR-449a	3.349 (1.788–6.274)	0.001	1.281 (0.338–4.862)	0.716
hsa-miR-214-3p	0.671 (0.367–1.226)	0.194		
hsa-miR-615-3p	1.153 (0.675–1.971)	0.602		
hsa-miR-144-5p	3.143 (1.544–6.359)	0.001	0.399 (0.104–1.534)	0.181
hsa-miR-3619-5p	1.354 (0.665–2.756)	0.403		
hsa-miR-34c-5p	1.695 (0.888–3.239)	0.110		

Multivariate logistic regression analysis was further adjusted for age, hypertension, diabetes mellitus, and log-transformed levels of hsa-miR-410-3p, hsa-miR-34a-5p, hsa-miR-1271-5p, hsa-miR-96-5p, hsa-miR-449b-5p, hsa-miR-449a and hsa-miR-144-5p.

Supplemental Table 3. Conservation of miR-344e/410-3p target sequences across species in the 3' UTR of *Ldlr*.

***Ldlr* 3' UTR**	
Homo sapiens (human)	5'-UGCCAGAGCUUUGUU**UUAUAU**AU-3'
Rattus norvegicus (rat)	5'-GCCCUGGGUCCUGUU**UUAUAU**AU-3'
Mus musculus (mouse)	5'-GCCCCAGGUUCUGUU**UUAUAU**AU-3'
Bos taurus (cow)	5'-UGCCAGAGCUUUGUU**UUAUAU**AU-3'
Macaca mulatta (Rhesus)	5'-UGCCAGAGCUUUGUU**UUAUAU**AU-3'
Pan troglodytes (Chimpanzee)	5'-UGCCAGAGCUUUGUU**UUAUAU**AU-3'
	||||||
miR-344e/410-3p	3'--**AAUAUA**--5'

Conserved bases are shown in bold text

Supplemental Table 4. Stem-loop primers for reverse transcription.

Primer name	Primer sequence
miR-615-3p	CCTGTTGTCTCCAGCCACAAAAGAGCACAATATTTCA GGAGACAACAGGAAGAGGG
miR-96-5p	CCTGTTGTCTCCAGCCACAAAAGAGCACAATATTTCA GGAGACAACAGGAGCAAAA
miR-1912-3p	CCTGTTGTCTCCAGCCACAAAAGAGCACAATATTTCA GGAGACAACAGGAGTTCTC
miR-344e-3p	CCTGTTGTCTCCAGCCACAAAAGAGCACAATATTTCA GGAGACAACAGGATAGTCA
miR-410-3p	CCTGTTGTCTCCAGCCACAAAAGAGCACAATATTTCA GGAGACAACAGGACAGGCC
miR-34b-5p	CCTGTTGTCTCCAGCCACAAAAGAGCACAATATTTCA GGAGACAACAGGACAATCA
miR-34c-5p	CCTGTTGTCTCCAGCCACAAAAGAGCACAATATTTCA GGAGACAACAGGGCAATCA
miR-214-3p	CCTGTTGTCTCCAGCCACAAAAGAGCACAATATTTCA GGAGACAACAGGACTGCCT
miR-144-5p	CCTGTTGTCTCCAGCCACAAAAGAGCACAATATTTCA GGAGACAACAGGACTTACA
miR-669e-5p	CCTGTTGTCTCCAGCCACAAAAGAGCACAATATTTCA GGAGACAACAGGATGAACA
miR-669f-3p	CCTGTTGTCTCCAGCCACAAAAGAGCACAATATTTCA GGAGACAACAGGATACGTG
miR-466e-3p	CCTGTTGTCTCCAGCCACAAAAGAGCACAATATTTCA GGAGACAACAGGTCTTATG
miR-466e-5p	CCTGTTGTCTCCAGCCACAAAAGAGCACAATATTTCA GGAGACAACAGGTATGTAC
miR-344b-1-3p	CCTGTTGTCTCCAGCCACAAAAGAGCACAATATTTCA GGAGACAACAGGACAGTCG
miR-331-5p	CCTGTTGTCTCCAGCCACAAAAGAGCACAATATTTCA GGAGACAACAGGAACAAAC
miR-466b-5p	CCTGTTGTCTCCAGCCACAAAAGAGCACAATATTTCA GGAGACAACAGGCATGGAC
hsa-miR-615-3p	CCTGTTGTCTCCAGCCACAAAAGAGCACAATATTTCA GGAGACAACAGGAAGAGGG
hsa-miR-96-5p	CCTGTTGTCTCCAGCCACAAAAGAGCACAATATTTCA GGAGACAACAGGAGCAAAA
hsa-miR-410-3p	CCTGTTGTCTCCAGCCACAAAAGAGCACAATATTTCA GGAGACAACAGGACAGGCC
hsa-miR-34a-5p	CCTGTTGTCTCCAGCCACAAAAGAGCACAATATTTCA GGAGACAACAGGACAACCA
hsa-miR-34c-5p	CCTGTTGTCTCCAGCCACAAAAGAGCACAATATTTCA

	GGAGACAACAGGGCAATCA
hsa-miR-214-3p	CCTGTTGTCTCCAGCCACAAAAGAGCACAATATTTCA
	GGAGACAACAGGACTGCCT
hsa-miR-144-5p	CCTGTTGTCTCCAGCCACAAAAGAGCACAATATTTCA
	GGAGACAACAGGCTTACAG
hsa-miR-449a	CCTGTTGTCTCCAGCCACAAAAGAGCACAATATTTCA
	GGAGACAACAGGACCAGCT
hsa-miR-449b-5p	CCTGTTGTCTCCAGCCACAAAAGAGCACAATATTTCA
	GGAGACAACAGGGCCAGCT
hsa-miR-1271-5p	CCTGTTGTCTCCAGCCACAAAAGAGCACAATATTTCA
	GGAGACAACAGGTGAGTGC
hsa-miR-3619-5p	CCTGTTGTCTCCAGCCACAAAAGAGCACAATATTTCA
	GGAGACAACAGGGCTGCAC
cel-miR-39-3p	CCTGTTGTCTCCAGCCACAAAAGAGCACAATATTTCA
	GGAGACAACAGGCAAGCTG

Supplemental Table 5. Real-time PCR primers in this study.

Primer name	Primer sequence	
miR-615-3p	Forward	CGGGCTCCGAGCCTGGGTCT
	Reverse	CAGCCACAAAAGAGCACAAT
miR-96-5p	Forward	CGCCGTTTGGCACTAGCACAT
	Reverse	CAGCCACAAAAGAGCACAAT
miR-1912-3p	Forward	CGGGCCACAGAACATGCAGT
	Reverse	CAGCCACAAAAGAGCACAAT
miR-344e-3p	Forward	CGGGCGATATAACCAAAGCC
	Reverse	CAGCCACAAAAGAGCACAAT
miR-410-3p	Forward	CGCCGAATATAACACAGAT
	Reverse	CAGCCACAAAAGAGCACAAT
miR-34b-5p	Forward	GCGGCAGGCAGTGTAATTAGC
	Reverse	CAGCCACAAAAGAGCACAAT
miR-34c-5p	Forward	GCGGCAGGCAGTGTAGTTAGC
	Reverse	CAGCCACAAAAGAGCACAAT
miR-214-3p	Forward	CGGGCACAGCAGGCACAGAC
	Reverse	CAGCCACAAAAGAGCACAAT
miR-144-5p	Forward	GCGGCGGATATCATCATATAC
	Reverse	CAGCCACAAAAGAGCACAAT
miR-669e-5p	Forward	CGGGCTGTCTTGTGTGTGCA
	Reverse	CAGCCACAAAAGAGCACAAT
miR-669f-3p	Forward	CGCCGCATATACATACACACA
	Reverse	CAGCCACAAAAGAGCACAAT
miR-466e-3p	Forward	GCGGCTATACATACACGCACA
	Reverse	CAGCCACAAAAGAGCACAAT
miR-466e-5p	Forward	CGGGCGATGTGTGTGTACAT
	Reverse	CAGCCACAAAAGAGCACAAT
miR-344b-1-3p	Forward	CGGGCGATATAACCAAAGCC
	Reverse	CAGCCACAAAAGAGCACAAT
miR-331-5p	Forward	GCGGCGGTCTTGTTTGG
	Reverse	CAGCCACAAAAGAGCACAAT
miR-466b-5p	Forward	CGGGCTATGTGTGTGTGTAT
	Reverse	CAGCCACAAAAGAGCACAAT
LDLR	Forward	TTAGGGACTGGCTATGGT
	Reverse	ACTGGCTGTGCTTGAAAT
U6	Forward	CTCGCTTCGGCAGCACATATACT
	Reverse	ACGCTTCACGAATTTGCGTGTC
GAPDH	Forward	TTAGGGACTGGCTATGGT
	Reverse	ACTGGCTGTGCTTGAAAT
hsa-miR-615-3p	Forward	GCGCTCCGAGCCTGGGTCT
	Reverse	CAGCCACAAAAGAGCACAAT
hsa-miR-96-5p	Forward	GCGCTTTGGCACTAGCACAT

	Reverse	CAGCCACAAAAGAGCACAAT
hsa-miR-410-3p	Forward	GCGCAATATAACACAGAT
	Reverse	CAGCCACAAAAGAGCACAAT
hsa-miR-34a-5p	Forward	GCGCTGGCAGTGTCTTAGC
	Reverse	CAGCCACAAAAGAGCACAAT
hsa-miR-34c-5p	Forward	GCGCAGGCAGTGTAGTTAGC
	Reverse	CAGCCACAAAAGAGCACAAT
hsa-miR-214-3p	Forward	GCGCACAGCAGGCACAGAC
	Reverse	CAGCCACAAAAGAGCACAAT
hsa-miR-144-5p	Forward	GCGCGGATATCATCATATA
	Reverse	CAGCCACAAAAGAGCACAAT
hsa-miR-449a	Forward	GCGCTGGCAGTGTATTGTT
	Reverse	CAGCCACAAAAGAGCACAAT
hsa-miR-449b-5p	Forward	GCGCAGGCAGTGTATTGTT
	Reverse	CAGCCACAAAAGAGCACAAT
hsa-miR-1271-5p	Forward	GCGCCTTGGCACCTAGCAA
	Reverse	CAGCCACAAAAGAGCACAAT
hsa-miR-3619-5p	Forward	GCGCTCAGCAGGCAGGCTG
	Reverse	CAGCCACAAAAGAGCACAAT
cel-miR-39-3p	Forward	GCGCTCACCGGGTGTAAAT
	Reverse	CAGCCACAAAAGAGCACAAT